

**AUTOMATED IDENTIFICATION AND DIFFERENTIATION OF SPECTRALLY SIMILAR HYDROTHERMAL MINERALS ON MARS.** B. P. Rasmussen<sup>1</sup>, B. L. Ehlmann<sup>1,2</sup>, E. Amador<sup>2</sup>, E. Rampe<sup>3</sup>

<sup>1</sup>Division of Geological & Planetary Sciences, California Institute of Technology, Pasadena, CA 91125 ([brasmuss@caltech.edu](mailto:brasmuss@caltech.edu)), <sup>2</sup>Jet Propulsion Laboratory, California Institute of Technology, Pasadena, CA 91109, <sup>3</sup>NASA Johnson Space Center, Houston, TX, 77058.

**Introduction:** Early telescopic observations corroborated hydration related absorptions on Mars in the infrared [1,2, etc.]. Images from the Viking missions led to speculation of hydrothermal alteration [3] and were followed by two missions which mapped the spatial variability of the  $\sim 3 \mu\text{m}$  hydration feature. [4,5]. Since then, the Compact Reconnaissance Imager for Mars (CRISM) [6] has provided high spatial resolution (up to 18m) spectral identification of a suite of hydrothermal and diagenetic minerals which have illuminated a range of formation mechanisms [7].

Presence/absence and spatial segregation or mixing of minerals like prehnite, epidote, chlorite amphiboles, and mixed-layer Fe/Mg smectite-chlorite provide valuable evidence for the geologic setting of deposits on Earth, and these phases are often used as temperature and aqueous chemistry indicators in terrestrial systems [e.g. 8, 9]. Mapping the distribution of these phases will help to answer whether Mars had widespread conditions favorable for low-grade metamorphism and diagenesis, or only focused hydrothermal systems in areas of high heat flow. Further characterizing the chemistry and structure of these phases will then help to answer how most of the widespread Fe/Mg phyllosilicates formed, further defining early geochemical cycling and climate.

A fully automated approach for accurate mapping of important hydrothermal mineral phases on Mars has been a challenge. Due to overlapping features in the M-OH region ( $\sim 2.2\text{-}2.4 \mu\text{m}$ ), the strongest absorption features of chlorite, prehnite, and epidote in the short-wave infrared are difficult to distinguish from one another [10] and from the most commonly occurring hydrated silicates on Mars, Fe/Mg smectites [7, 11]. Weaker absorptions are present in both prehnite and epidote which help to distinguish them from chlorite and smectites, but their relative strength in the presence of noise and spatial mixing is often too low to confidently identify them without the noise suppression and feature enhancement methods described here. The spectral signatures of mixed-layer Fe/Mg smectite-chlorite and partially chloritized Fe/Mg smectites [12] have not yet been adequately assessed. Here we evaluate the effectiveness of two empirical and statistical methods for identifying and differentiating these phases using CRISM data.

**Methods:** Multiple methods derived from past work are combined for noise removal and feature enhancement starting from ENVI CRISM Analysis Toolkit (CAT) preprocessed (photometric and volcano scan corrections) images subsetted to 1.3-2.6  $\mu\text{m}$  wavelengths. Initial despiking and spurious pixel removal as described by Carter et al. [11] and adapted in [13] are applied before principle component analysis is used to transform the dataset, and twenty components are maintained for an inverse transform. These twenty components generally represent over 99.9% of the spectral variability of a CRISM image, and the discarded components are mostly stochastic noise [e.g. 14]. After an initial iteration of destriping, denominator spectra for ratioing are identified as by [13] to emphasize absorption features, and a final destriping is performed. This results in the final data product used for spatial mapping. Two methods are tested for detection and spatial mapping: Factor Analysis/Target Transformation (FA/TT), and mineral-specific empirical scoring functions.

The twenty eigenvectors from the forward PC transform are used for FA/TT, where a set of library spectra are fit using a least-squares inverse method. Past projects have shown FA/TT's ability to detect small, poorly defined exposures of spectrally distinct minerals with CRISM data [e.g. 14]. Plots of the target transformation (detection) are generated and the spectral angle distance to both the library spectrum and each pixel of the scene (spatial mapping) are calculated. The merit for the FA/TT method is that it is designed to be sensitive to the occurrence of minerals, even when only present in mixtures [14].

The benefit of empirical scoring functions is traceability to observable diagnostic spectral parameters. For prehnite and epidote, the first OH-stretch overtones occur at  $\sim 1.47 \mu\text{m}$  and 1.54-1.56  $\mu\text{m}$ , respectively. When combined with their M-OH absorptions near 2.35-2.36  $\mu\text{m}$ , these features uniquely identify the minerals. The empirical prehnite score here uses a combination of tightly bounded band depths at 1.473  $\mu\text{m}$  ( $2\nu(\text{OH})$ ) and 2.238  $\mu\text{m}$  (M-OH) to avoid interference from other mineral phases in the M-OH region and from atmospheric water near 1.5  $\mu\text{m}$ . The epidote scoring function uses band depths centered at 1.55  $\mu\text{m}$  ( $2\nu(\text{OH})$ ) and 1.83  $\mu\text{m}$  (a

characteristic but unattributed absorption present in many library and published spectra) [e.g. 11,15]. The two band depths in each case are scaled relative to each other based on library spectra and summed together to produce the final score, a unitless value for each pixel (spatial mapping). The highest scoring (top 0.1%) pixels with a BD 2.33-2.36  $\mu\text{m}$  absorption present ( $\text{BD} > 0.003$ ) are extracted and evaluated against library spectra for goodness of fit (detection). Scoring functions for other minerals are in progress.

The pipeline was applied to two CRISM images with previously identified prehnite/epidote/chlorite. FRT000096CA is from the northern plains, and FRT0000B1B5 is from Toro crater near Nili Fossae. 96CA shows part of a complex crater noted to have a chlorite/epidote/prehnite occurrence [13]. B1B5 captures prehnite/chlorite in the central peak and floor of a complex crater with origin due to crustal excavation [16] or post-impact hydrothermalism [17].

**Preliminary Results:** In B1B5, prehnite is mapped unambiguously with the scoring function, correlating well with BD2.33-2.36  $\mu\text{m}$  (Fig. 1 B,C). A small absorption near 2.25  $\mu\text{m}$ , and a sequence of multiple, overlapping absorptions near  $\sim 1.4 \mu\text{m}$  (see automatically extracted spectrum, E, black) indicate that prehnite is mixed with another hydrated silicate with a 2.25  $\mu\text{m}$  absorption, most likely chlorite. Unmixed chlorite is not apparent in any pixel. This is illustrated by the ubiquitous nature of the 1.47 and 2.23  $\mu\text{m}$  features wherever a 2.33-2.36  $\mu\text{m}$  absorption is present. Target transformation (blue spectrum, E) matches prehnite well and successfully reconstructs the weak 1.47 and 2.23  $\mu\text{m}$  features. While epidote score mapping is noisy and extracted spectra unconvincing (D), its target transformation fits the library spectrum moderately well, replicating the 1.55  $\mu\text{m}$ , 1.83  $\mu\text{m}$ , and 2.36  $\mu\text{m}$  features sufficiently, but missing the 2.26  $\mu\text{m}$  feature present in the library spectrum entirely (E).

In 96CA, despite the 2.33-2.36  $\mu\text{m}$  feature being very weak (note color bar scale in H), the prehnite score is spatially coherent for the mound features at the bottom left of the image (G, I). The automatically extracted spectrum shows a 2.23  $\mu\text{m}$  shoulder, and a very weak 1.47  $\mu\text{m}$  feature, while target transformation shows a moderately good fit to prehnite (K). Epidote empirical scoring is elevated in one of the mounds as well (J), and target transformation also shows a moderate fit, although lacking some characteristics of the main absorption (L). If prehnite/epidote are present in the extracted spectra from the mounds in 96CA, a broad M-OH feature with a significant  $\sim 2.32 \mu\text{m}$  component combined with a  $\sim 1.4 \mu\text{m}$  feature in both suggests dominantly Fe/Mg smectites and/or Mg-chlorite.

**Future Work:** Our refinement of techniques for automated detection and discrimination of prehnite,

chlorite, and epidote is ongoing to assess accuracy in detection. We will also develop spectral standards and scoring for mixed layer chlorite-smectites.

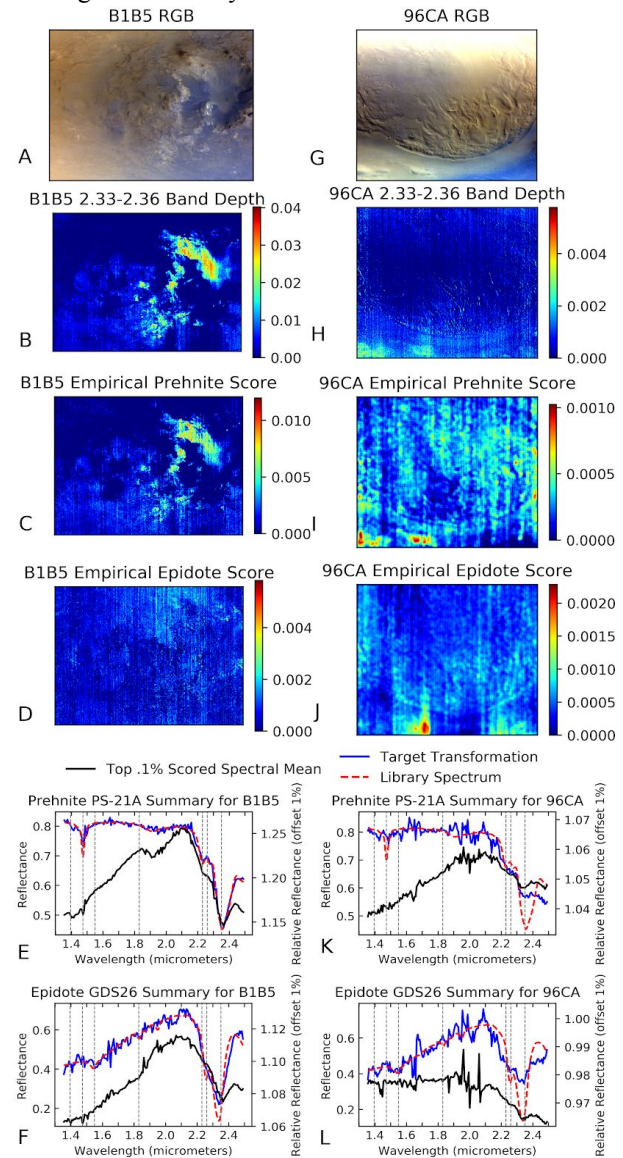


**Figure 1:** (A,G) Approximate true color RGBs. (B-D, H-J) Empirical scores for prehnite and epidote. Panels I/J are smoothed with an 11x11 median. Note the correlation between BD2.33-2.36 and score images. (E,F,K,L) detection spectra from FA/TT and empirical scoring methods.

**Acknowledgments:** This work will be conducted under funding from NASA Solar System Workings #80NSSC18K1535 (PI E. Rampe) and NASA MDAP #NNH18ZDA001N, (Science PI E. Amador/PI Ehlmann)

**References:** [1] Sinton, *Icarus*, 1967 [2] Beer et al., *Icarus* 1971. [3] Singer et al., *JGR:SE*, 1979. [4] Bibring et al., *Nature*, 1989. [5] Milliken et al., *JGR:P*, 2007. [6] Murchie et al., *JGR:P*, 2007. [7] Ehlmann and Edwards, *AnnRev EaPS*, 2014. [8] Rae, *NewZ GT WS*, 2011. [9] Inou et al., *Res Geo*, 2010. [10] White et al., *Geoc: E,E,A*, 2017. [11] Carter et al., *PSS*, 2013. [12] V.M. Tu et al., *LPSC*, 2019. [13] Pan et al., *JGR:P*, 2017. [14] Amador et al., *Icarus*, 2018. [15] Kokaly et al., *USGS*, 2017. [16] Ehlmann et al., *JGR:P*, 2009. [17] Marzo et al., *Icarus*, 2010.